$BaNi_2V_2O_8$: A two-dimensional honeycomb antiferromagnet

N. Rogado,[1] Q. Huang,[2] J. W. Lynn,[2] A. P. Ramirez,[3] D. Huse,[4] and R. J. Cava[1]
[1]*Department of Chemistry and Princeton Materials Institute, Princeton University, Princeton, New Jersey 08544*
[2]*NIST Center for Neutron Research, National Institute of Standards and Technology, Gaithersburg, Maryland 20899*
[3]*Department of Thermal Physics, Los Alamos National Laboratory, Los Alamos, New Mexico 87545*
[4]*Department of Physics, Princeton University, Princeton, New Jersey 08544*
(Received 10 July 2001; revised manuscript received 22 October 2001; published 4 April 2002)

The magnetic properties of $BaNi_2V_2O_8$ are reported. The magnetic Ni ions are arranged in a two-dimensional (2D) honeycomb net. Susceptibility, specific heat, and neutron diffraction measurements reveal the onset of antiferromagnetic long-range ordering (LRO) close to 50 K. Diffuse scattering that is characteristic of strong 2D magnetic correlations are observed up to 100 K. $\chi(T)$ of $Ba(Ni_{1-x}Mg_x)_2V_2O_8$ ($0 \leqslant x \leqslant 0.2$) shows the gradual disappearance of LRO with doping.

DOI: 10.1103/PhysRevB.65.144443 PACS number(s): 75.30.−m, 75.50.Ee, 75.40.Cx

I. INTRODUCTION

The discovery of materials that display quasi-one-dimensional (1D) or quasi-two-dimensional (2D) magnetic properties has made possible the verification and refinement of theoretical models for such systems. The geometry of the magnetic lattice plays a key role. Exchange coupling in low-dimensional systems based on spin-$\frac{1}{2}$ 1D chains and 2D square lattices has been extensively studied due to their importance in understanding high-T_c superconductivity. Low-dimensional magnetic lattices based on triangles, in particular of the frustrating *kagomé* geometry,[1–3] have been of significant recent interest. Another variant of a triangle-based system is the honeycomb net. The few studies on the properties of compounds based on this lattice have exhibited interesting properties such as spin glass behavior,[4] spin-flop transition,[5] Kosterlitz-Thouless behavior,[6] and even superconductivity.[7,8]

Here we report the characterization of the magnetic properties of a spin-1 honeycomb compound, $BaNi_2V_2O_8$. $BaNi_2V_2O_8$ (space group $R-3$; $a=5.0375$ and $c=22.3300$ Å) (Ref. 9) is a 2D compound that consists of honeycomb layers of edge-sharing NiO_6 octahedra (Fig. 1). The layers are separated by nonmagnetic $V^{5+}O_4$ tetrahedra and Ba^{2+} ions. The magnetic properties are therefore expected to be dominated by antiferromagnetic (AFM) Ni^{2+}-O-Ni^{2+} interactions within the layers. Since Ni^{2+} in octahedral coordination has the e_g^2 configuration, $BaNi_2V_2O_8$ is a spin-1 magnetic system.

$BaNi_2V_2O_8$ is isostructural with $BaM_2X_2O_8$ ($M=$Co, Ni; $X=$P, As), whose magnetic properties have been previously reported.[10–12] $BaNi_2P_2O_8$ and $BaNi_2As_2O_8$ are considered to be prototypes of a 2D *XY* system. Here we find that in spite of the structural resemblance, the magnetic properties of $BaNi_2V_2O_8$ are quite different from the other nickel compounds. The bulk magnetic susceptibility $\chi(T)$ and specific heat $C(T)$ of $BaNi_2V_2O_8$ show very subtle features at around 50 K indicative of magnetic ordering, barely seen in high-resolution measurements. Three-dimensional (3D) ordering is confirmed by neutron diffraction to occur at that temperature. In contrast, for $BaNi_2P_2O_8$ and $BaNi_2As_2O_8$, the 3D ordering transition is clearly visible in the $\chi(T)$ and $C(T)$ plots. Also, unlike the other members of this family, the spins in the current compound appear to lose all but an extremely small amount of their entropy before the 3D ordering transition. Both the structural and magnetic properties of $BaNi_2V_2O_8$ suggest that it may be considered as one of the best candidates on which to test the theoretical predictions for a 2D *XY* model. Mg-doped samples of $BaNi_2V_2O_8$ were prepared and characterized to investigate the effect of substituting nonmagnetic ions into the magnetic Ni sites.

II. EXPERIMENT

Polycrystalline samples of $Ba(Ni_{1-x}Mg_x)_2V_2O_8$ ($0 \leqslant x \leqslant 0.2$) were synthesized by conventional solid-state reaction using $BaCO_3$, NiO, MgO, and V_2O_5 as starting materials. The reagents were mixed in stoichiometric proportion and heated in dense Al_2O_3 crucibles at 950 °C in air for 2 days with intermediate grindings. The powder samples were pressed into pellets and heated in dense Al_2O_3 crucibles at 1000 °C in air for 18 h. Single crystals of $BaNi_2V_2O_8$ were grown via a self-flux technique. A mixture of the starting materials was heated at 1100 °C in air for 4 h and then slowly cooled to room temperature. The yellow hexagonal plates of $BaNi_2V_2O_8$ were then mechanically separated from the flux.

Powder x-ray-diffraction (XRD) with Cu $K\alpha$ radiation was employed to characterize the samples. The magnetic susceptibility data were obtained for the powder samples between 300–5 K at applied fields of 1 T using a Quantum Design PPMS magnetometer. The anisotropic magnetization data were obtained on single crystals using a Quantum Design MPMS superconducting quantum interference device magnetometer. Specific heat measurements were performed on a sintered powder sample of $BaNi_2V_2O_8$ using a standard semiadiabatic heat-pulse technique.

The neutron powder diffraction intensity data of $BaNi_2V_2O_8$ were collected using the BT-1 high-resolution powder diffractometer at the NIST Center for Neutron Research, employing a Cu (311) monochromator to produce a monochromatic neutron beam of wavelength 1.5401 Å. Collimators with horizontal divergences of 15′, 20′, and 7′ arcs were used before and after the monochromator, and after

 ©2002 The American Physical Society

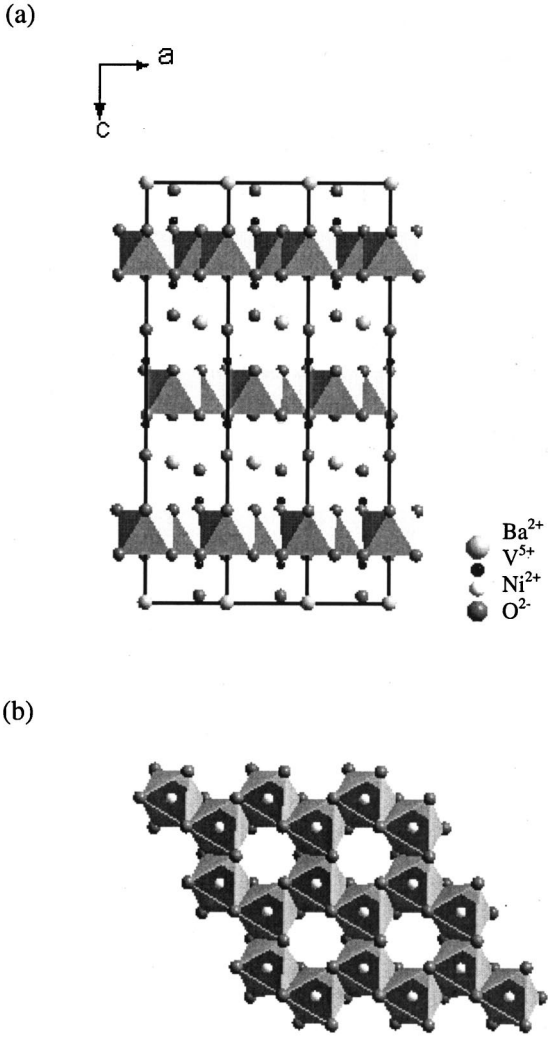

FIG. 1. (a) Crystal structure of $BaNi_2V_2O_8$. (b) The magnetic Ni^{2+} ions (located at the center of the octahedra) are shown arranged in honeycomb layers.

the sample, respectively. The intensities were measured in steps of 0.05° in the 2θ range 3°–168°. Data were collected at room temperature and 8 K. The structural parameters were refined using the program general structure analysis system.[13] The neutron-scattering amplitudes used in the refinements were 0.525, 1.03, −0.0382, and 0.581 ($\times 10^{-12}$ cm) for Ba, Ni, V, and O, respectively. Additional data were obtained on the high-intensity BT-7 triple-axis spectrometer to explore the magnetic scattering in more detail. For these measurements, a pyrolytic graphite PG(002) double monochromator was employed at a wavelength of 2.46 Å, with $52'$ collimation after the sample and no analyzer.

III. RESULTS AND DISCUSSION

The structure refinement for a 10-g powder sample of $BaNi_2V_2O_8$ at 295 K was carried out successfully using previously reported structural parameters[9] as initial values. The crystal structure was found to be hexagonal (space group $R-3$) with $a=5.028\,99(4)$ and $c=22.3450(2)$ Å. Less than four percent of an impurity phase in this sample was identified to be a tetragonal phase with the symmetry $14_1/acd$ reported for $Ba_{0.5}Sr_{0.5}Ni_2V_2O_8$ (Ref. 14) and was taken into consideration in the final refinements. No structural phase transitions were found from room temperature to 8 K. Because of the very small coherent neutron-scattering length for V, the z coordinate for V was fixed at 0.424 58,[9] and its temperature factor was fixed. The final structural parameters and selected interatomic distances are given in Table I.

The susceptibility $\chi(T)$ of polycrystalline single-phase $BaNi_2V_2O_8$ (Fig. 2) exhibits a very broad peak near 125 K, which is indicative of low-dimensional ordering. A small tail is observed at low temperatures due to the presence of small quantities of magnetic impurities. No obvious feature associated with long-range ordering (LRO) can be observed. The high temperature series expansion (HTSE) for an $S=1$ 2D honeycomb antiferromagnet has been theoretically derived by Rushbrook and Wood,[15] and can be used to fit the $\chi(T)$ data for $BaNi_2V_2O_8$. The expression is

$$\chi_{\mathrm{AFM}}=(Ng^2\mu_B^2/3kT)[S(S+1)](1+Ax+Bx^2+Cx^3+Dx^4+Ex^5+Fx^6)^{-1}, \quad (1)$$

where $x=|J|/kT$, J is the exchange interaction between Ni sites, $k=1.3807\times10^{-16}$ erg K^{-1}, N is Avogadro's constant, $\mu_B=9.274\times10^{-21}$ erg G^{-1}, $A=4$, $B=7.333$, $C=7.111$, $D=-5.703$, $E=-22.281$, and $F=51.737$. A good fit to the high temperature experimental $\chi(T)$ data (150–300 K) was obtained with two fitting parameters, as shown in Fig. 2, yielding $J/k=-48$ K and $g=2.3$. The exchange parameter values reported for $BaNi_2P_2O_8$ and $BaNi_2As_2O_8$ are $J/k\sim-8$ and $J/k\sim-(6-7)$ K,[10] respectively. Comparison to $J/k=-48$ K for $BaNi_2V_2O_8$ confirms quantitatively that the Ni^{2+}-Ni^{2+} AFM interactions within the planes of $BaNi_2V_2O_8$ are much stronger than those in the phosphate and arsenate, making it a more ideal candidate for 2D behavior than the other compounds.

Measurement of the susceptibilities parallel ($\chi_\parallel$) and perpendicular ($\chi_\perp$) to the c axis on single crystals of $BaNi_2V_2O_8$ give evidence for planar anisotropic behavior (Fig. 3). At high temperatures, the compound behaves isotropically and becomes anisotropic near 100 K. A very small feature is observed at ~48 K in $\chi_\parallel(T)$ (inset, Fig. 3). The anisotropic magnetization data suggest that the spins lie in the plane of the Ni-O honeycomb layers. The reported susceptibilities for the related compounds $BaNi_2X_2O_8$ (X = P, As) also imply strong planar character, consistent with their layered structure. However, unlike $BaNi_2V_2O_8$, $BaNi_2P_2O_8$ and $BaNi_2As_2O_8$ clearly display significant features in $\chi(T)$ associated with 3D spin ordering: broad maxima at $T(\chi_{\max})\sim32$ K and inflection points ($\delta^2\chi/\delta T^2=0$) at the Néel temperatures $T_N=24.5\pm1$ and $T_N=19\pm2$ K, respectively, marking the 3D ordering transitions.[10]

$BaNi_2X_2O_8$ (X = V, P, As) are isostructural, consisting of (001) magnetic layers wherein the Ni^{2+} ions are arranged in honeycomb layers. For $BaNi_2V_2O_8$, the Ni^{2+}-Ni^{2+} distance within the honeycomb planes ($d_1=a/\sqrt{3}$) is 2.90 Å while the

TABLE I. Structural parameters of $BaNi_2V_2O_8$ at 295 K (first line) and 8 K (second line). The space group is $R\bar{3}$ (148). The magnetic unit cells are $a_M = b_M = a_N$ and $c_M = 2c_N$, where the a_N and c_N are the nuclear cell constants. The z coordinate and temperature factor for V were fixed (see text).

	$a_N = 5.028\,99(4)$ Å 25.02049(2) (Å)		$c_N = 22.3450(2)$ Å 22.2381(3) (Å)		$V = 489.41(1)$ Å^3 485.42(1) Å^3	
Atom	x	y	z		B (Å^2)	
Ba	0	0	0		0.86(5)	
	0	0	0		0.36(5)	
Ni	0	0	0.169 57(6)		0.53(2)	
	0	0	0.169 65(7)		0.28(2)	
V	0	0	0.424 58		0.56	
	0	0	0.424 58		0.24	
O(1)	0	0	0.349 94(9)			
	0	0	0.349 16(9)			
O(2)	0.6590(3)	0.0047(3)	0.219 65(4)			
	0.6598(3)	0.0060(3)	0.219 68(4)			
	B_{11}	B_{22}	B_{33}	B_{12}	B_{13}	B_{23}
O(1)	0.99(4)	$=B_{22}$	1.14(6)	0.40(2)	0	0
	0.43(4)	$=B_{22}$	0.96(7)	0.21(2)	0	0
O(2)	0.54(4)	0.55(5)	1.41(5)	0.28(5)	0.16(5)	0.12(6)
	0.35(4)	0.20(5)	0.90(3)	0.13(5)	0.11(5)	0.07(5)
R_p (%):	3.89	R_{wp} (%): 5.01	χ: 1.66			
	4.65	6.07	2.13			

Selected interatomic distances (Å)

	295 K	8 K
Ba-O(1)	2.9271(3)	2.9197(2)
Ba-O(2)	3.020(1)	3.006(1)
Ni-O(2)	2.058(1)	2.051(1)
Ni-O(2)	2.056(2)	2.048(2)
V-O(1)	1.668(2)	1.677(2)
V-O(2)	1.743(1)	1.745(1)
Ni-Ni	2.9064(1)	2.9016(1)

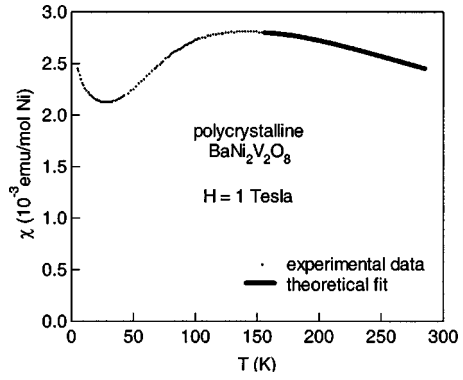

FIG. 2. Temperature dependence of the magnetic susceptibility of polycrystalline $BaNi_2V_2O_8$. The experimental data (open circles) is shown together with the theoretical fit (solid line) for an $S=1$ 2D honeycomb model. Applied dc field is 1 T.

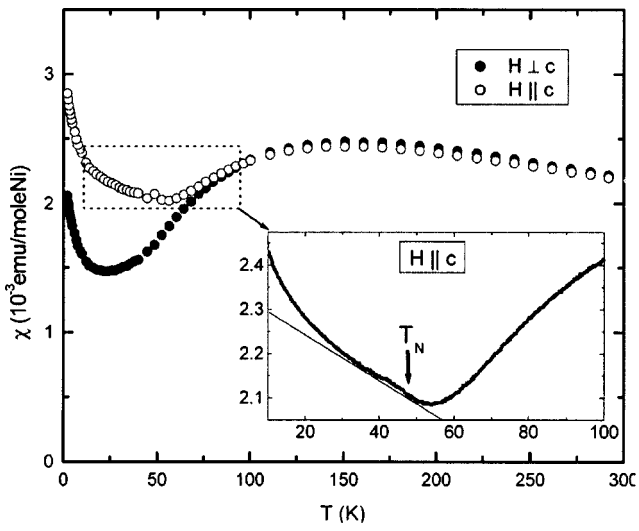

FIG. 3. Temperature dependence of the susceptibilities $\chi_\perp$ and $\chi_\parallel$ of $BaNi_2V_2O_8$. Inset shows a plot of $\chi_\parallel(T)$ from 10–100 K. The solid line is a guide to the eye.

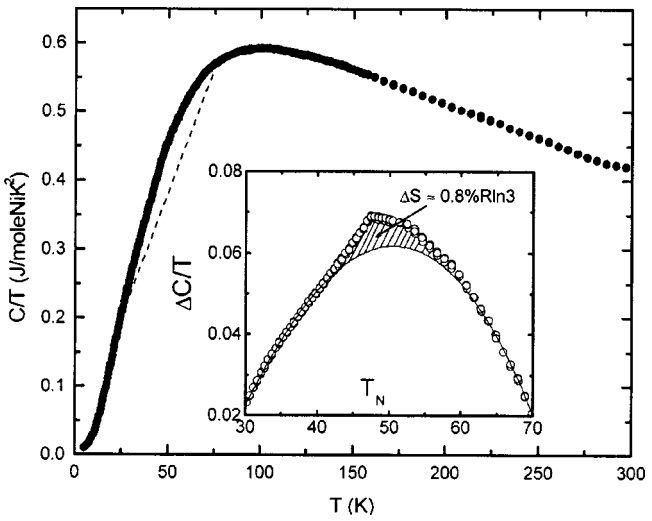

FIG. 4. The temperature dependence of the specific heat of $BaNi_2V_2O_8$ represented as C/T vs T. Inset shows a plot of ΔC vs T from 25–75 K, with a broken line in the main panel taken as C_0 in $\Delta C=(C_{\rm obs}-C_0)$. The line representing C_0 is arbitrary and is taken for purposes of illustrating the weak feature in C vs T near 50 K.

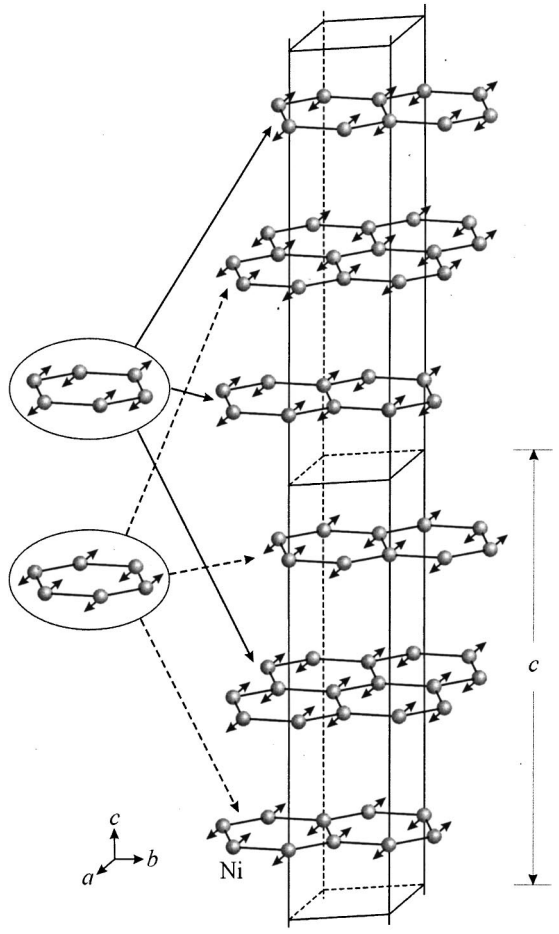

FIG. 5. The magnetic structure of $BaNi_2V_2O_8$. For simplicity, only the Ni atoms are shown.

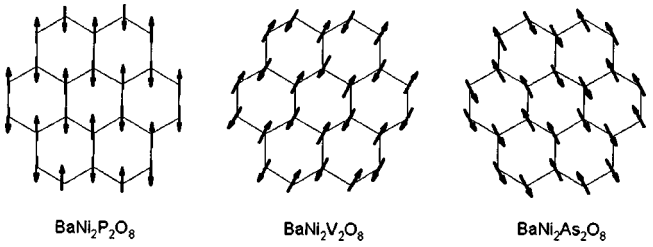

FIG. 6. The magnetic structures of $BaNi_2X_2O_8$ (X=P, V, As).

interlayer distance ($d_2=c/3$) is 7.45 Å. Thus, we expect a pronounced 2D magnetic character in this system from the large interlayer-to-intralayer ratio $d_2/d_1=2.57$. When compared to $BaNi_2X_2O_8$ (X=P, As) with $d_2/d_1\sim 2.8$,[10] the value obtained for $BaNi_2V_2O_8$ is smaller but it is not too different. The Ni-O-Ni bond angles, which are important to magnetic superexchange, can also be compared. The bond angles for $BaNi_2V_2O_8$ (Ref. 9) are found to be 90.00(19)°, while those for $BaNi_2P_2O_8$ (Ref. 16) and $BaNi_2As_2O_8$ (Ref. 17) are 84.95(19)° and 86.99(2)°, respectively, which are less than the 90° Ni-O-Ni bond angle expected for ideal edge-sharing octahedra. The Ni-O-Ni superexchange interaction is expected to be very sensitive to this angle. This slight difference in bond angles may be responsible for the observed weaker intralayer coupling and more favored 3D ordering in the phosphate and arsenate.

Specific heat measurements on $BaNi_2V_2O_8$ were also taken. The magnetic specific heats for the analogous isostructural $BaNi_2X_2O_8$ (X=P, As) exhibit large, sharp λ-type anomalies at T_N,[18] marking a significant loss of entropy at the 3D ordering transition. The specific heat data for

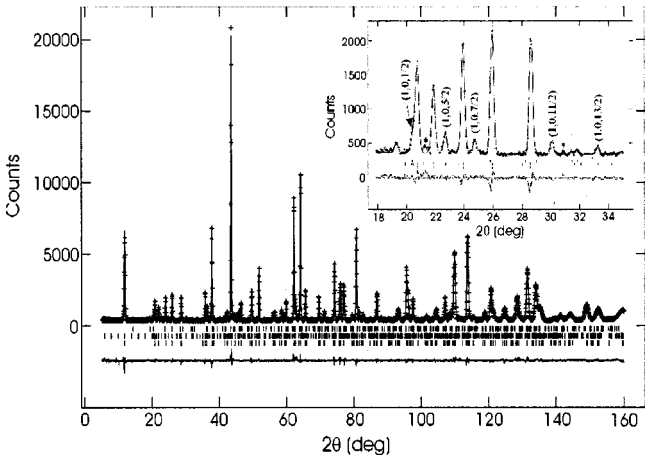

FIG. 7. Observed (cross), calculated (solid line), and difference neutron-diffraction profiles for $BaNi_2V_2O_8$ at 8 K. The vertical lines show the reflection positions of the nuclear peaks (bottom), magnetic peaks (middle), and the impurity phase (top). The inset shows the details of the magnetic peaks, fit with the magnetic model shown in Fig. 5. The weak peaks at ~21.2° and ~30.7° are due to a small amount (<0.5%) of an (unknown) impurity phase. (These peaks are not seen in the BT-7 data, where a different wavelength was used, because of poor resolution; the two peaks overlap with the nearest strong peaks.)

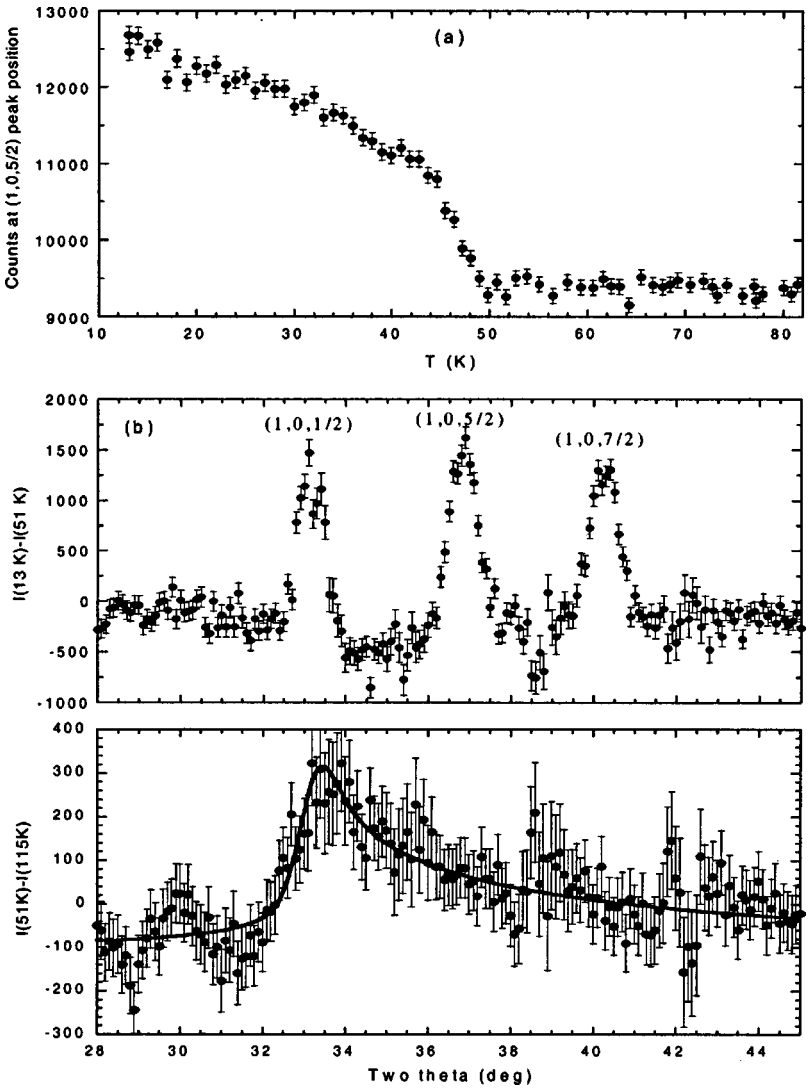

FIG. 8. Magnetic diffraction data obtained on the BT-7 triple-axis spectrometer. (a) Peak intensity of the (1 0 $\frac{5}{2}$) magnetic reflection (counts/4 min) as a function of the temperature, indicating an antiferromagnetic phase transition at $T_N = 50$ K. (b) Three-dimensional magnetic Bragg peaks obtained from subtracting the data at 51 K from the data at 13 K (counts/2 min). (c) The difference of the data obtained at 51 K, just above the three-dimensional ordering temperature, from the data obtained at 115 K (counts/2 min). The asymmetric line shape is characteristic of strong two-dimensional correlations. The curve is a fit assuming no correlations between planes, and correlations that are resolution limited within the plane. (Note: The extra scattering at 30° is due to a structural peak from an impurity.)

$BaNi_2V_2O_8$ are shown in Fig. 4. They do not show any sharp transition associated with long-range magnetic ordering, but only a very broad peak near 100 K. High-resolution measurements, however, show that a very small feature in ΔC vs T may be seen at ~48 K (inset), which is the same temperature at which a small feature appears in $\chi_{\|}(T)$. The total entropy needed to fully disorder a mole of a spin-1 system is $R \ln 3$. However, the entropy change at the transition temperature for $BaNi_2V_2O_8$ was calculated to be ~0.8% $R \ln 3$. This extremely small change in entropy at the 3D transition temperature suggests that the magnetic entropy is lost over a very wide temperature range upon spin ordering, that is, most of the entropy of the system has been lost during the transition to a 2D ordered state at $T > 50$ K.

Neutron diffraction data on $BaNi_2V_2O_8$ confirm the existence of 3D ordering at low temperatures. The magnetic peaks can be indexed using the $\mathbf{k} = (1\ 0\ \frac{1}{2})$ propagation vector (doubling the unit cell in the c direction). The AFM structure model shown in Fig. 5 provides a very good fit to the observed magnetic peaks. This long-range ordered magnetic structure is very similar to that of $BaNi_2P_2O_8$ (Ref. 18) (Fig. 6). On the other hand, the magnetic structure of $BaNi_2As_2O_8$ is quite different from the other two compounds; it can be considered to be characterized by ferromagnetic chains that are coupled antiferromagnetically.[10] In the magnetic model for $BaNi_2V_2O_8$, each Ni^{2+} spin lies within the honeycomb layer and is aligned antiferromagnetically with its three nearest Ni^{2+} neighbors. The Ni^{2+} spins between layers are also arranged antiferromagnetically along the c axis. The ordered magnetic moment for Ni refines to $1.55(4)\mu_B$ and lies in the ab plane. This moment is less than the expected value of $2\mu_B$ for an antiferromagnetically ordered spin-1 compound, which may be attributed to quantum fluctuations. The observed and calculated intensities of the final refinement are shown in Fig. 7.

To investigate the magnetic ordering in more detail, data were collected on BT-7 and are shown in Fig. 8. A plot of the peak intensity of the (1 0 $\frac{5}{2}$) magnetic reflection, which is proportional to the square of the ordered antiferromagnetic moment, is shown in Fig. 8(a) as a function of temperature. The data indicate a sharp AFM phase transition at $T_N = 50(1)$ K. The data in Fig. 8(b) reveal three magnetic peaks, obtained by subtracting the observed scattering at 13 K from the ''background'' scattering observed at 51 K. In

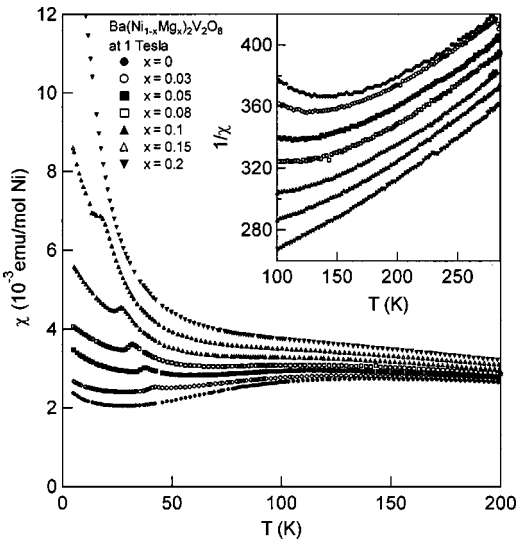

FIG. 9. $\chi(T)$ of polycrystalline $Ba(Ni_{1-x}Mg_x)_2V_2O_8$ ($0 \leqslant x \leqslant 0.2$). The inset shows a plot of $1/\chi$ vs T from 100–300 K.

particular, there is no magnetic intensity observed at positions where the nuclear peaks are located. However, the data suggest that there are still substantial magnetic correlations just above the 3D ordering temperature. To investigate this further, in Fig. 8(c) we show the subtraction of the data at 51 K from the scattering at 115 K, which is well above the ordering temperature. The observed asymmetric line shape reveals that strong 2D correlations exist above the 3D ordering temperature,[19,20] and we therefore conclude that the exchange interactions within the layers are considerably stronger than the interactions between layers. The solid curve in the figure is a least-squares fit to a 2D profile, assuming a Lorentzian correlation function within the plane, and no correlations between planes. The results of the fit indicate that the correlations within the planes are resolution limited at this temperature (just above T_N), and we estimate a lower limit of ~150 Å for the correlation length with this instrumental resolution. Typically single crystals are necessary to obtain more detailed information,[20] and it will be very interesting to investigate the spin dynamics in this material if larger single crystals become available.

The effect of doping nonmagnetic Mg^{2+} ions into the hexagonal Ni-O layer was investigated. The magnetic-susceptibility data for polycrystalline $Ba(Ni_{1-x}Mg_x)_2V_2O_8$ ($0 \leqslant x \leqslant 0.2$) are shown in Fig. 9. It is clearly seen in the figure that substituting Mg^{2+} for Ni^{2+} resulted in a dramatic increase in the susceptibility at low temperatures, which increases with Mg content, indicative of the creation of free spins in the honeycomb lattice through the introduction of nonmagnetic ions into the Ni sites. The increasing low temperature $\chi(T)$ eventually masks the weak 150 K peak. It is notable that the high temperature $\chi(T)$ also increases with doping. The highest temperature $\chi(T)$ data plotted as $1/\chi$ vs T (inset) indicate that the temperature is insufficiently high enough to observe the behavior associated with free spins by simply fitting to the Curie-Weiss law. However, the Curie constant C may be estimated by treating the susceptibility at high temperatures as a sum of two terms: (i) a Curie term

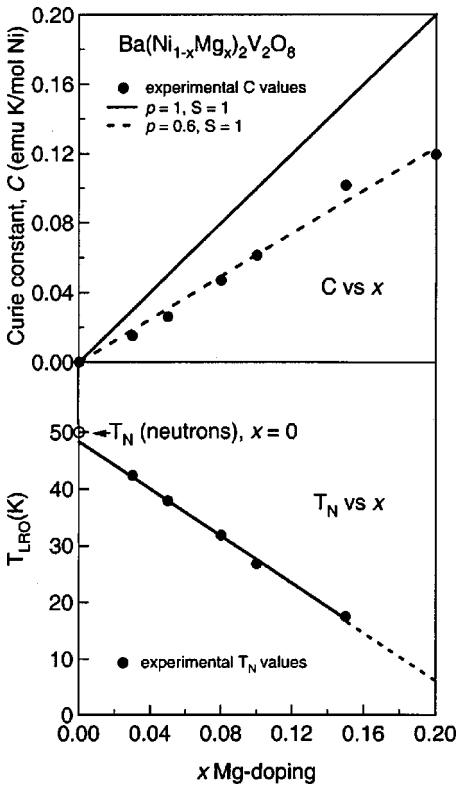

FIG. 10. Plots of (a) Curie constants (C) and (b) the long-range-ordering temperatures (T_{LRO}) of $Ba(Ni_{1-x}Mg_x)_2V_2O_8$ vs the amount (x) of Mg doping estimated from the susceptibility data.

arising from the presence of free spins, and (ii) χ_{AFM} coming from the HTSE for a 2D honeycomb antiferromagnet given by Eq. (1):

$$\chi = p(C/T) + \chi_{AFM}, \tag{2}$$

where p is the fraction of free spins per substituted Ni site. The above equation was fitted to the $\chi(T)$ data from 150–300 K and gave reasonable values for the Curie constants. C is plotted against x in Fig. 10 (upper panel). Simplistically, we assume that every Mg^{2+} ($S=0$) ion substituted into a Ni^{2+} ($S=1$) site should give rise to *one* $S=1$ spin in the honeycomb layers. As shown in the figure, the experimentally obtained Curie constants are smaller than the simple prediction (represented by the solid line). However, the experimental values are shown to give a linear fit to a situation wherein each mole of nonmagnetic dopant creates only 60% $S=1$ spin, shown by the broken lines in the figure. This is reasonable to expect since the random introduction of nonmagnetic sites into the honeycomb layers probably results not only in the formation of paramagnetic spins but also to correlated spins as well, which tend to suppress the total moment.

A more striking observation is that the Mg doping results in the small feature that appears below 50 K in the $\chi_{\|}(T)$ of $BaNi_2V_2O_8$ becoming more distinct (Fig. 9). The reason why the dilution allows the transition to appear in the uniform magnetization has been discussed in the literature in the context of diluted Ising antiferromagnets.[21] In the pure system,

the ordered magnetization is precisely equal and opposite on the two sublattices, such that a uniform field does not couple to it. But with dilution, this precise balance is randomly disrupted, allowing the uniform field to couple randomly to the order parameter and pick up a feature due to the onset of the ordering that now shows up in the $\chi(T)$ plot. It can also be observed from Fig. 9 that this LRO peak shifts to lower temperatures with increasing Mg content. Figure 10 (lower panel) shows how the LRO transition temperature (T_{LRO}) is related to the degree of doping. The decrease in the LRO temperature with doping suggests that the dilution effect increases as free spins are introduced by substituting nonmagnetic Mg^{2+} into the Ni sites, consistent with what is expected. This leads to the weakening of the Ni-Ni antiferromagnetic interactions and the eventual disappearance of LRO with $\chi(T)$ behaving more like Curie-Weiss for $x \geqslant 0.2$.

IV. CONCLUSION

$BaNi_2V_2O_8$ is a 2D spin-1 honeycomb antiferromagnet. Although isostructural with $BaNi_2X_2O_8$ ($X=$P, As), it displays quite different magnetic properties. Magnetic measurements show that the exchange interactions within the layers are considerably stronger than the interactions between layers, which makes this compound an ideal candidate for a 2D *XY* model. Neutron diffraction data also show that strong 2D correlations exist well above the 3D ordering temperature. Substituting nonmagnetic Mg^{2+} ions into the magnetic lattice results in the release of spins from the ordered state and the appearance of distinct LRO peaks in the susceptibility. Detailed characterization of the crossover from the 2D to 3D ordering transition will be of considerable interest, as would a detailed investigation of the spin correlations in the 2D regime.

ACKNOWLEDGMENTS

This research was supported by the National Science Foundation (NSF) through the MRSEC program (NSF MRSEC Grant No. DMR-9809483). We would like to thank Tom Clinton for his assistance with the fits for the two-dimensional magnetic correlations.

[1] R. J. Cava, A. P. Ramirez, Q. Huang, and J. J. Krajewski, J. Solid State Chem. **140**, 337 (1998).
[2] A. P. Ramirez, B. Hessen, and M. Winklemann, Phys. Rev. Lett. **84**, 2957 (2000).
[3] C. H. Booth, J. S. Gardner, G. H. Kwei, R. H. Heffner, F. Bridges, and M. A. Subramanian, Phys. Rev. B **62**, 755 (2000).
[4] M. Bieringer, J. E. Greedan, and G. M. Luke, Phys. Rev. B **62**, 6521 (2000).
[5] D. J. Goossens, A. J. Studer, S. J. Kennedy, and T. J. Hicks, J. Phys.: Condens. Matter **12**, 4233 (2000).
[6] H. M. Rønnow, A. R. Wildes, and S. T. Bramwell, Physica B **276–278**, 676 (2000).
[7] S. Shamoto, T. Kato, Y. Ono, Y. Miyazaki, K. Ohoyama, M. Ohashi, Y. Yamaguchi, and T. Kajitani, Physica C **306**, 7 (1998).
[8] R. Weht, A. Filipetti, and W. E. Pickett, Europhys. Lett. **48**, 320 (1999).
[9] R. Wichmann and H. Müller-Buschbaum, Rev. Chim. Miner. **21**, 824 (1984).
[10] L. P. Regnault and J. Rossat-Mignod, in *Magnetic Properties of Layered Transition Metal Compounds*, edited by L. J. de Jongh (Kluwer, Dordrecht, 1990), and references therein.
[11] L. P. Regnault, J. Rossat-Mignod, J. Y. Henry, and L. J. De Jongh, J. Magn. Magn. Mater. **31–34**, 1205 (1983).
[12] L. P. Regnault, J. Rossat-Mignod, J. Y. Henry, R. Pynn, and D. Petitgrand, in *Magnetic Excitations and Fluctuations*, edited by S. W. Lovesey, U. Balucani, F. Borsa, and V. Tognetti (Springer-Verlag, Berlin, 1984).
[13] A. C. Larson and R. B. Von Dreele, Los Alamos National Laboratory Report No. LAUR086-748, 1990.
[14] M. von Postel and H. Müller-Buschbaum, Z. Anorg. Allg. Chem. **615**, 97 (1992).
[15] G. S. Rushbrook and P. J. Wood, Mol. Phys. **1**, 257 (1958).
[16] B. El-Bali, M. Bolte, A. Boukhari, J. Aride, and M. Taibe, Acta Crystallogr., Sect. C: Cryst. Struct. Commun. **55**, 701 (1999).
[17] S. Eymond, A. Durif, and C. Martin, C. R. Acad. Sci., Ser. C **268**, 1694 (1969).
[18] L. P. Regnault, J. Y. Henry, J. Rossat-Mignod, and A. De Combarieu, J. Magn. Magn. Mater. **15–18**, 1021 (1980).
[19] H. Zhang, J. W. Lynn, W. H. Li, T. W. Clinton, and D. E. Morris, Phys. Rev. B **41**, 11 229 (1990); H. Zhang, J. W. Lynn, and D. E. Morris, *ibid.* **45**, 10 022 (1992).
[20] T. W. Clinton, J. W. Lynn, Z. J. Liu, Y. X. Jia, T. J. Goodwin, R. N. Shelton, B. W. Lee, M. Buchgeister, M. B. Maple, and J. L. Peng, Phys. Rev. B **51**, 15 429 (1995); J. W. Lynn, T. W. Clinton, W-H. Li, R. W. Erwin, J. Z. Liu, K. Vandervoort, R. N. Shelton, and P. Klavins, Phys. Rev. Lett. **63**, 2606 (1989).
[21] S. Fishman and A. Aharony, J. Phys. C **12**, L729 (1979).